Journal of Visualization, Vol. 6, No. 3 (2003) 225-234

Chemically Reacting Liquid Round Jet

Hong, S. D.*[1], Okamoto, K.*[1], Kim, H. J. *[2], Sugii, Y. *[1] and Madarame, H. *[1]

*1 Nuclear Engineering Research Laboratory, University of Tokyo, Tokai-mura, Ibaraki, 319-1188, Japan.
e-mail: hong@utnl.jp
*2 Ajou University, Div. of Mechanical Industrial Engineering, Paldal-Gu, Suwon 442-749, Korea

Received 1 October 2002
Revised 5 December 2002

Abstract : An experimental study was conducted on a chemically reacting liquid round free jet. The Laser Induced Fluorescence (LIF) technique was adopted to evaluate the mixing suppression of the jet into liquid streams. The jet profiles were quantitatively evaluated for both the upstream region near the transition point and the downstream region far away from the transition point, and comparisons were conducted between the reacting and the non-reacting jet cases. In the downstream region, the jet profiles for the two cases were found to be quite different. It was concluded that the occurrence of a chemical reaction affects the momentum diffusion of the jet in the downstream region, which results in these differences.

Keywords : Chemical reaction, LIF, Mixing suppression, Momentum diffusion, Transition point.

1. Introduction

Chemical reactions frequently occur in fluid engineering. Because the generation of chemically reacting jets can produce explosions in reactors, it is important to investigate the characteristics of these reacting jets in order to safely design industrial reactors. In sodium-cooled nuclear reactors, for example, sodium-water reactions inside the steam generator are one of the primary causes of accidents. A number of studies have reported on the characteristics of mixing enhancement in fluid flow. Breidenthal (1981) discovered that the amount of the chemical product was independent of the Reynolds number and at most only weakly dependent on the Schmidt number. Koochesfahani *et al.* (1986) measured the passive scalar by using the probability density functions at the transition stage of the mixing layer. Bennani *et al.* (1985) and Nagata *et al.* (2000) reported on the reaction of two chemicals inside the grid turbulence. They proposed a type of dimensionless parameter called the Damköhler number.

Conversely, Sasaki (2000) reported on the mixing suppression in a turbulent shear flow caused by a chemical reaction. He measured the pH distribution on the chemically reacting jet flow, which ranged from 4.0 to 5.5, using the Dual Emission LIF technique. The authors

(Okamoto *et al.,* 2000; Hong *et al.*, 2001) reported that the chemical reaction affected the liquid round jet's mixing suppression. The results from the LIF images showed that the liquid round free jet's diffusion of momentum was suppressed when a chemical reaction was present, when compared with a non-reaction jet.

Since chemical reactions only occur on the very thin interface layers, they can be expected to be substantial on a large interface area of the downstream region. In this study, laser induced fluorescence (LIF) has been utilized to investigate the influences of a chemical reaction far downstream from the transition point The diffusions of the liquid round free jet were visualized.

2. Experiments

The Laser Induced Fluorescent technique (LIF) is one of the most useful visualization methods to reveal the nature of a fluid flow. This technique was used to investigate the momentum diffusion of a jet into an ambient fluid, when a chemical reaction was occurring. Figure 1 shows the schematic of the experimental setup. The test section, having a 100 mm x 100 mm cross section, was made from an acrylic resin. A stainless steel nozzle, with a 23 cm length and a 2 mm inner diameter D, was horizontally installed at the center of the test section. In the presented experiment condition, the hydrodynamic entry length is less than 10 cm. So, the velocity profiles at the nozzle exit are fully developed. The flow rates of both the ambient flow and the jet flow were controlled by their respective control valves. An electric heater was used to maintain the temperature of the fluid, and the feedback signals of a digital thermometer were used to control the temperature with accuracy of the order of 0.1° C. Rhodamine B was selected as the LIF dye, and it was solved into the jet fluid only. Its concentration was set to 0.85 mg/L.

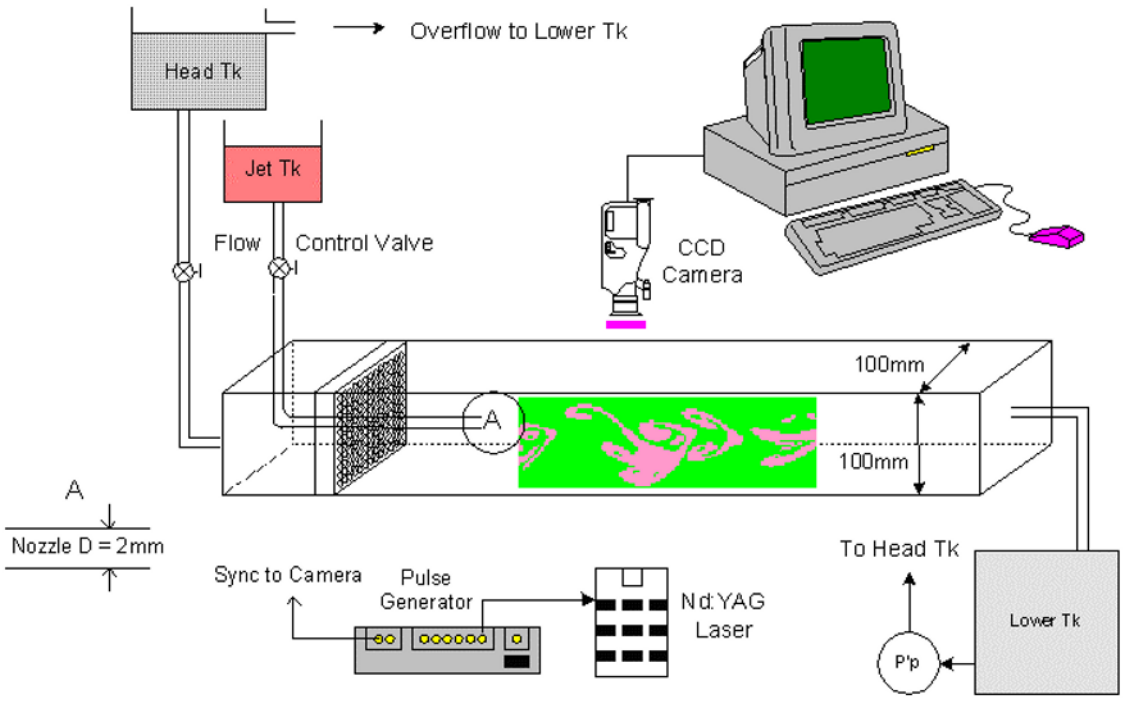

Fig. 1. Experimental setup.

This fluorescent dye absorbs a specific 532 nm wavelength from a Nd:YAG laser. It then emits specific 580 nm wavelength fluorescent light (orange color). Only above 560 nm wavelength fluorescent intensity through the long pass filter was detected by CCD camera. The 1mm laser light sheet illuminated a two-dimensional vertical plane in the center of the jet flows, the CCD camera, synchronized with the laser illumination by the pulse generator, captured the illuminated area. The image was captured by the CCD camera with 1024 × 1024 pixels of resolution at 10 frames/second. In order to detect only the fluorescent light and filter out unnecessary laser scattering light from the LIF image, a high pass optical filter was installed on the front of the CCD camera.

The combination of the ambient fluid and the jet fluid types are shown in Table 1. R refers to a reaction case, and the N denotes a non-reaction case. Ammonium hydroxide and acetic acid chemically reacted in the test section for cases R1 to R4. Equation 1 shows the equation for the reaction between the ammonium hydroxide and the acetic acid.

$$CH_3COOH + NHOH_4 \rightarrow CH_3COONH_4 + H_2O \quad (1)$$

Table 1. Experimental cases.

Case	Ambient fluid	Jet fluid --(pH)
R1	Acetic Acid (0.1 mol/L)	Ammonium hydroxide (0.01 mol/L)—11.0
R2	Acetic Acid (0.1 mol/L)	Ammonium hydroxide (0.05 mol/L) —11.0
R3	Acetic Acid (0.1 mol/L)	Ammonium hydroxide (0.1 mol/L) —11.0
R4	Acetic Acid (0.1 mol/L)	Ammonium hydroxide (0.5 mol/L) —11.0
N1	Water	Acetic Acid (0.1 mol/L) and Ammonium hydroxide (0.1 mol/L) —5.6
N2	Water	Acetic Acid (0.1 mol/L) —2.8
N3	Water	Ammonium hydroxide (0.1 mol/L) —11.0
N4	Water	Water—7.2

The reacting factor for the above reaction is k = 10^8 $m^3/(mol \cdot s)$ (Nagata et al., 2000). Above reaction is 13.8 kcal exothermic reaction. But this heat generating reaction increases an order of 10^{-6} degrees over the interface region for the low chemical species concentration. The effect of heat generation can be negligible. Case N4, water jet into water flow, was used as the reference. To clarify the effects of the jet solutions, an acetic acid jet and an ammonium hydroxide jet were separately injected into water. In case N1, two different chemicals were mixed in the jet tank before injection. The concentration of the jet fluid in the reacting cases was varied between 0.01 mol/L and 0.5 mol/L. For all the experiments the ambient fluid velocity was set to V_a = 5 mm/s.

In order to evaluate the effects of the chemical reaction on the mixing characteristics of the jet quantitatively, LIF images were analyzed for each experiment.

3. Results and Discussions

3.1 Transition Point

Figure 2 shows the images for the ammonium hydroxide jet into acetic acid case (R3). Figure 3 depicts the temporal images for the water jet into water case, N4, for three different Reynolds numbers: (a) 600, (b) 700, and (c) 800. The length of the visualized area was a distance of 10D to 28D away from the nozzle exit. Because the fluorescent dye was dissolved only in the jet fluid, the white high intensity area denotes the jet fluid and the black low intensity area depicts the ambient fluid. Rhodamine B fluorescence intensity is known to be not pH dependent over pH ranges 6 (Sasaki 2000, Coppeta et al., 1998). The fluids flow from the left to the right, as indicated by the horizontal arrow.

The interface between the jet flow and the ambient flow in the upstream region does not show vortices (stable). However, the interface of downstream jet region begins to show vortices (unstable) as jet flow down from upstream. It can be seen that the starting points of the unstable condition for both the reaction and non-reaction cases move upstream as the Reynolds number increases. For example, the starting point of the unstable region in Fig. 2 (a) is 18D away from the nozzle exit. In Fig. 2 (b) and 2 (c), however, the transition points move to left by 3D and 6D, respectively, when compared to Fig. 2 (a). In these figures, the Reynolds numbers increase from 600 to 800. Similarly, the transition points in the non-reaction case in Figure 3 advance farther upstream when the Reynolds number is increased. From the above instantaneous temporal images, one important observation related to the transition is that the fluctuation of jet flows appeared as a sinusoidal form and very variable. Therefore, it is necessary to determine the transition points from the temporal average images.

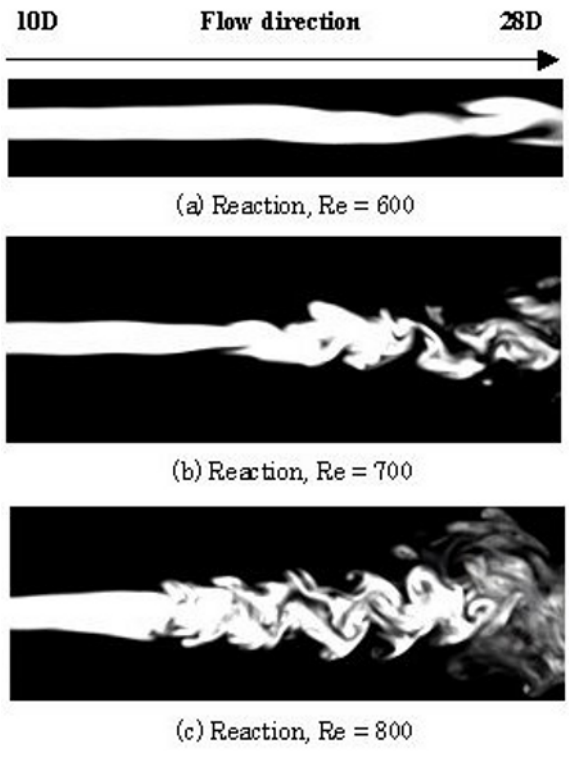

Fig. 2. Temporal images of the Reaction cases.

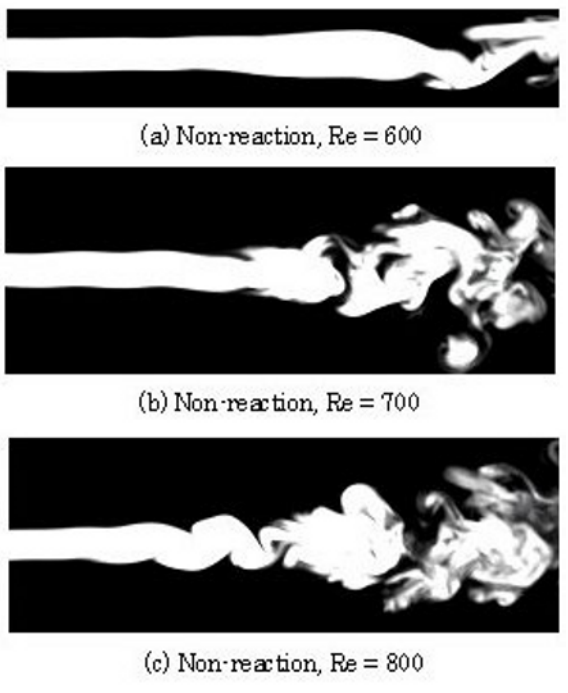

Fig. 3. Temporal Images of the Non-reaction cases.

In this experiment, 300 sequential instantaneous images were averaged before plotting the transition point. Figure 4 shows the relationship between the Reynolds number and the normalized transition points (x/D). The Reynolds numbers ranged from 400 to 1000 for both the R3 reaction case and the N4 non-reaction case. The Reynolds numbers were altered by changing the jet velocity. The fluid temperature was kept at 20° C. In the figure, the x-axis denotes the Reynolds number of the jet, and the y-axis indicates the distance, normalized by the nozzle inner diameter, between the transition point and nozzle exit. From the calibration images, the representative length D was determined to be equal to 53 pixels. The transition point at each Reynolds number was evaluated 10 times from 10 different temporal averaged images. The deviation of the transition point values in each time was within ± 1D. The red line in Figure 4 denotes the case of the ammonium hydroxide jet into the acetic acid, and the blue colored line represents the water jet into water case. The transition points for both cases moved upstream from about 22D to 7D as the Reynolds number of the jet was increased from 400 to 1000. Even though transition points for both cases continued to move upstream with an increase in the Reynolds number, the difference in the transition points for the two cases at the same Reynolds number was very small. This difference between the two cases is within the deviation ranges, which means that the chemical reaction does not considerably affect the location of the transition points in the flows.

It is well known that the Reynolds number is a function of the kinematic viscosity. An additional experiment was conducted by varying the temperature of the liquids. The relationship between the transition point (x/D) and the temperature, for both the R3 reaction case and the N4 non-reaction case, are shown in Fig. 5. The Reynolds number was held constant at 700 and the temperature was varied between 15° C and 25°C. The transition points for both cases moved downstream from approximately 8D to 15D as temperature was increased from 15°C to 25°C. This characteristic indicates that the shear force on the jet-ambient flow interface decreased as the temperature increased. From the figure it appears that the transition point of the reaction case is shifted slightly downstream, when compared with the non-reaction case. However, as in the Reynolds number variation experiment, the differences between the two results are within the deviation ranges. When the Reynolds number is relatively small, the large velocity gradient increases the growth rate of the Kelvin-Helmholtz instability. Therefore, as the Reynolds number is increased, the transition point advances upstream.

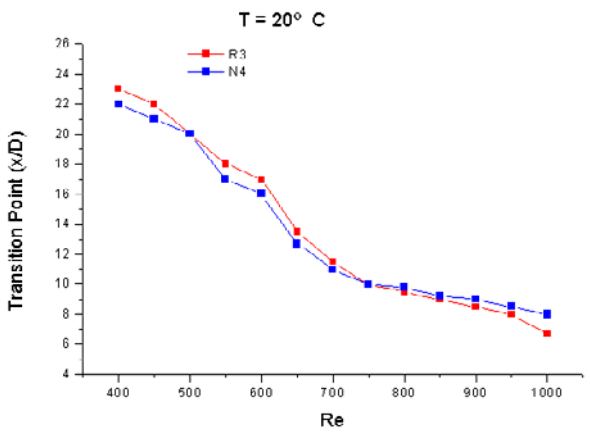

Fig. 4. Relationship between transition point and Re.

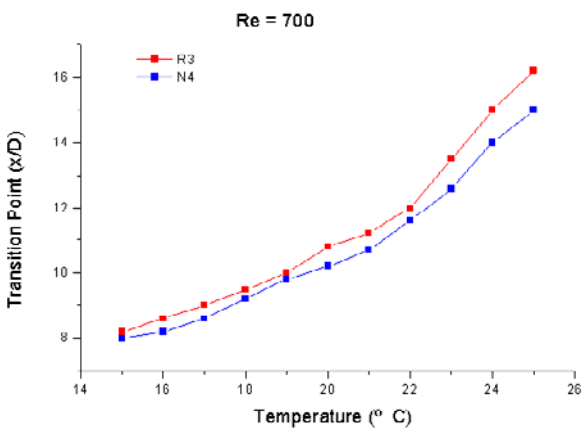

Fig. 5. Relationship between transition point and temp.

3.2 Downstream Region

As described in the previous section, the transition point was approximately the same for both the reacting and non-reacting cases. After the transition point, however, the jet diffusion was different for the two cases when using a half-width evaluation (Hong *et al.*, 2001). Because of this characteristic, the test area for the downstream region was selected far away from the transition point in order to investigate the mixing phenomena more precisely.

Figure 6 shows the temporal instantaneous images for the downstream jet flow for all of the experimental cases. For the experiments, the temperature was maintained at 14ºC and the Reynolds number set to 500. The nozzle exit was located at a distance of 37D upstream from the left-hand side of the test area. The length of the visualized area was 37D to 51D away from the nozzle exit. The vortex caused by the Kelvin-Hhelmholtz instability is clearly visible in the reacting cases. In non-reacting cases, however, the vortices had already become the complex turbulent flow.

It can be seen from Fig. 6 that the interface area between the jet flow and the ambient flow is very different between the reacting and non-reacting cases. Even though these experimental images are two-dimensional, it is apparent that the reacting case interface area is very narrow, but the non-reacting case interface area is very wide, relative to each other. Since the actual jet flows are in three-dimensions, the total difference of the interface areas may be significantly larger. This characteristic indicates that the momentum diffusion for the reacting case was suppressed more than for non-reacting case.

These instantaneous images provide temporal information of the jet flow. The suppressed momentum diffusion phenomenon was evaluated by using the specific jet width definition on these temporal images. The entire image intensity field is subtracted by the proper threshold values in order to eliminate background noise. The highest and lowest vertical jet location was determined, and the distance between these two points in the vertical direction was defined as the jet width for this study. Using this specific jet width method, the temporal instantaneous images were processed.

Figure 7 shows the histograms of the normalized jet width (w/D) values obtained from the 300 temporal instantaneous images for each experimental case. The threshold intensity value was set to 50, the x-axis was normalized by the jet width (w/D), and the y-axis was normalized by the number of images. Even though the ammonium hydroxide concentration was varied in the different reacting cases, it had little effect on the normalized jet width. This indicates that even a very small amount of ammonium hydroxide affects the amount of mixing suppression for the chemically reacting jet. There are, however, some differences in the results for the different non-reacting cases. While over 90% of the normalized jet width values for the reacting cases are less than 4, the jet width values for the non-reacting cases are widely distributed. The histogram of the ammonium hydroxide and acetic acid jet into water flow case was similar to that of the water jet into water flow case. The fact that the distribution of diffused jet widths is considerably different between the reacting and non-reacting cases indicates that the chemical reaction strongly affects the momentum diffusion of the chemically reacting jet in the downstream region far away from the transition point.

In order to confirm the reliability of the results, the experiment was repeated 10 times for the water jet into water flow case under the same experimental conditions. In order to obtain the average jet width value, 300 temporal instantaneous images were used. The normalized average minimum jet width value and the maximum jet width value were found to be 7.68D and 10.18D, respectively. Since the standard deviation of this experiment was ± 0.80D and the jet width values of the reacting and non-reacting cases were quite different, it was concluded that this jet

width definition, which uses temporal instantaneous images, is accurate enough to evaluate the jet mixing suppression of the jet due to the chemical reaction.

From Fig. 2, 3 and 6, it can be seen that the difference in the jet widths between the reacting cases and the non-reacting cases in the downstream region is much larger than in the upstream region. Because the liquid round free jet in the downstream region has grown considerably, it has a wider interface with the ambient fluid, and the effect of the chemical reaction in this region is larger. Consequently, the large effect of the chemical reaction is considered to magnify the difference of the jet widths in the downstream region.

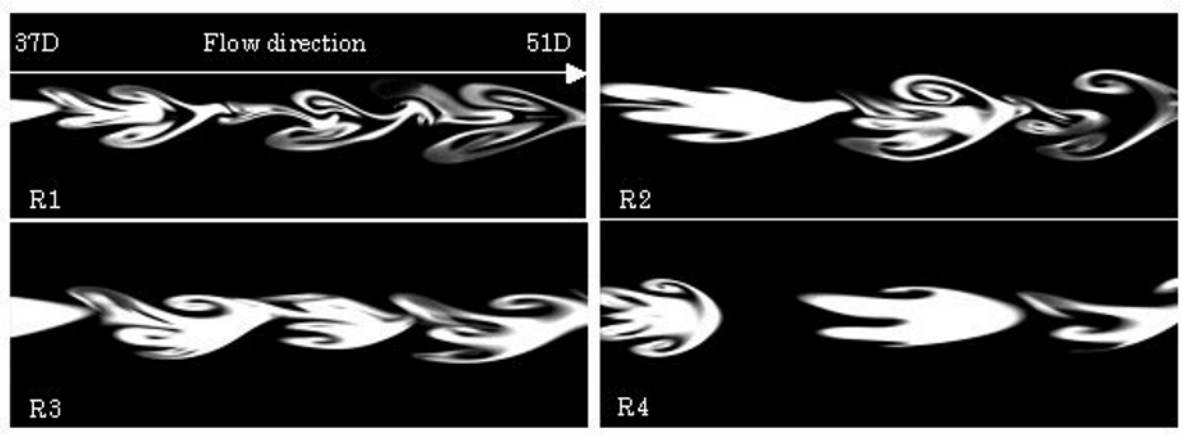

(a) Reacting cases

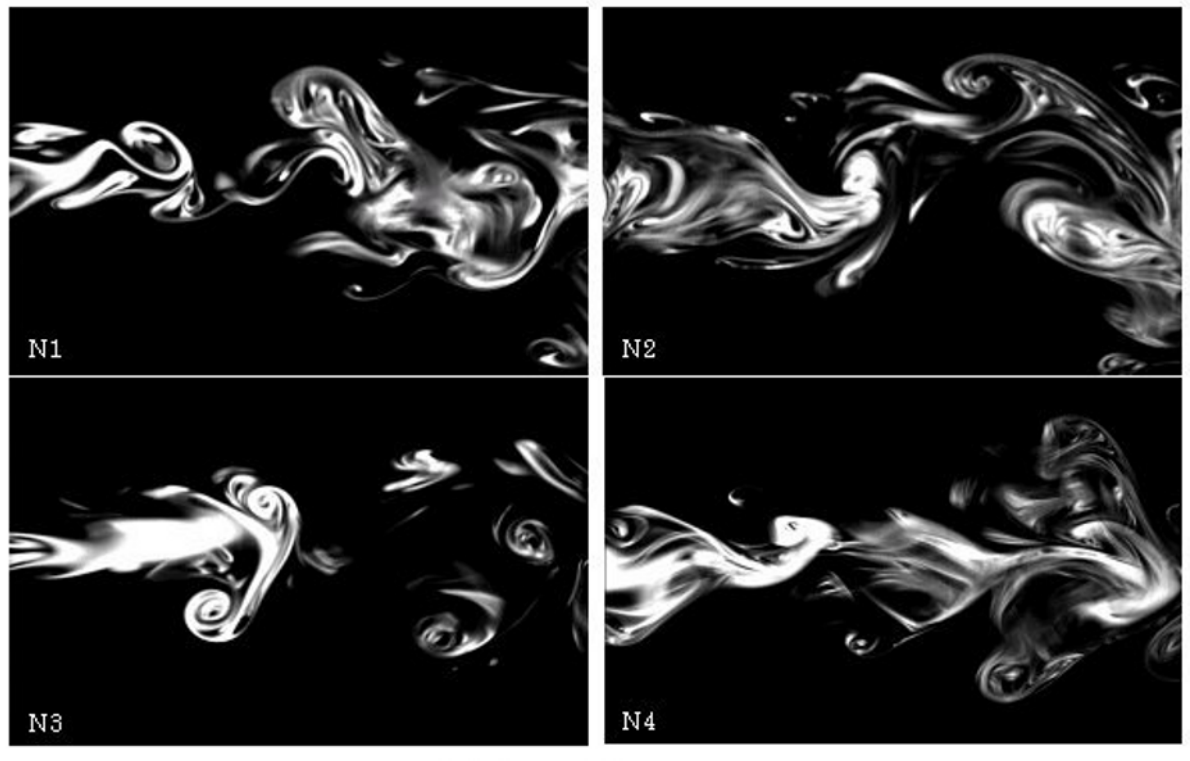

(b) Non-reacting cases

Fig. 6. temporal instantaneous images for Re = 500.

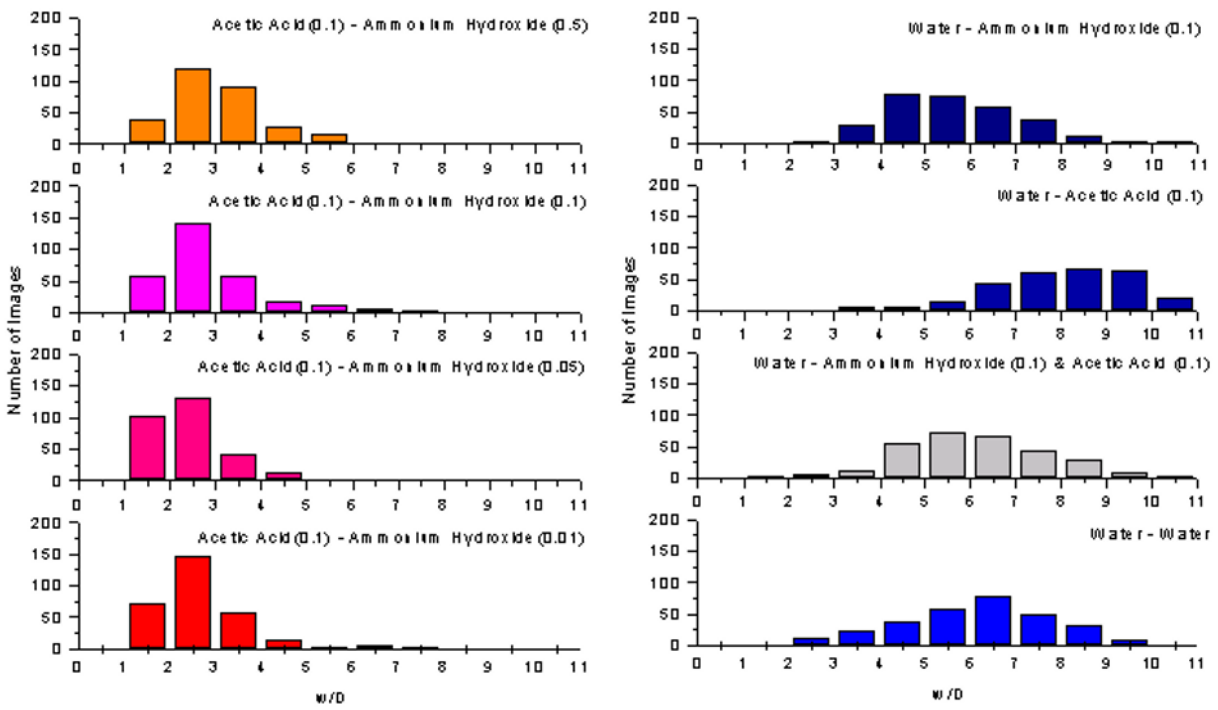

(a) Reacting case (b) Non-reacting case

Fig. 7. The histogram of jet width (w/D) for temporal images.

3.3 Mixing Suppression

Fig. 8 shows the sequential images at times t_0 and $t_0 + 100$ ms. From the calibration, it was calculated that the 2 mm nozzle diameter corresponds to 68 pixels in the images. In the reacting case, a vortex identified at time t_0 grew a little bit larger as it moved downstream. The red arrow in the figure identifies the vortex at t_0 and $t_0 + 100ms$. In the non-reacting case, however, the jet at $t_0 + 100$ ms has become quite different because the flow has already become the complex turbulent flow. As seen in Fig. 8 (a), vortex shapes can be distinguished and followed through the sequential images, as indicated by the red arrow. The velocity of a moving axial vortex can be calculated by comparing sequential temporal images. At the nozzle exit, the jet velocities for the two cases was set to 292 mm/s. However, after traveling 39D downstream, the velocity of moving vortex in the ammonium hydroxide jet into the acetic acid case and the water jet into the water case were calculated to be 88 mm/s and 45 mm/s, respectively. Even though the positions were not exactly coincident, the velocity of the moving vortex for the reacting case was about two times faster than the one for the non-reacting case.

In Fig. 8 (a), the ammonium hydroxide jet into the acetic acid flow case, the diffusion of the jet is suppressed and the axial velocity is as fast as the amount of suppressed diffusion. On the other hand, in the water jet into water case shown in Fig. 8 (b), the axial velocity reduces as the momentum is diffused.

From the results of these experiments, a chemical reaction was identified as having an influence on the characteristics of a liquid round jet. Because the chemical reaction occurs at the jet interface, a future quantitative and precise investigation should be extended to interface region of the jet in order to establish the root causes of these results.

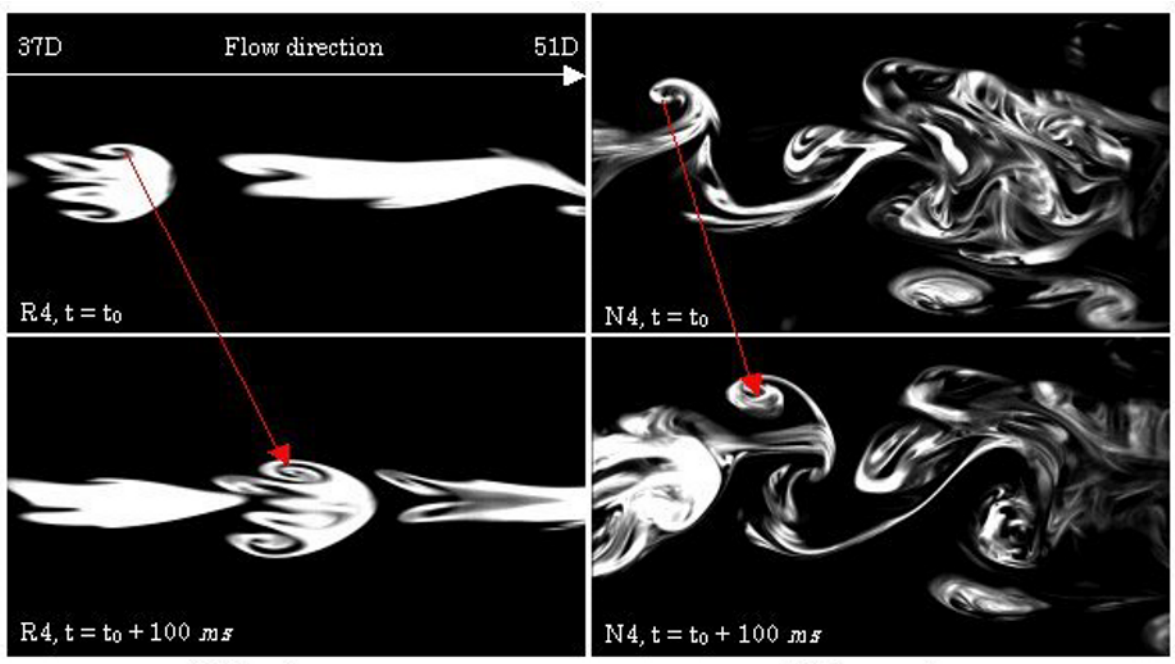

(a) Reacting case (b) Non-reacting case

Fig. 8. Sequential images for R4 and N4, Re = 500.

4. Conclusions

An experimental study was conducted on a chemically reacting liquid round free jet in order to investigate the influence of a chemical reaction on the characteristics of the jet. LIF images were used to provide comparisons between the momentum diffusion in reacting and non-reacting jet cases. The profile of the upstream region near the transition point did not reveal any distinguishable differences between the two cases. In the downstream region far from the transition point, however, the jet profiles for the reacting and non-reacting cases were quite different. The reason is that since the jet interface in the downstream region is wider than in the upstream region, the influence of the chemical reaction becomes lager in the downstream region. Moreover, the velocity of the moving vortices in the reacting case was faster than that in the non-reacting case due to the mixing suppression. The results showed that although the differences in the jet profiles in the upstream region were small, the momentum diffusion of the jet in the downstream region was clearly suppressed by the chemical reaction.

References

Bennani, A., et al., The Influence of a Grid Generated Turbulence in the Development of Chemical Reactions *AIChE J.,* 31 (1985), 1157-1166.

Breidenthal R., Structure in Turbulent Mixing Layers and Wakes using a Chemical Reaction, *J.* Fluid Mech., 109 (1981), 1-24.

Coppeta, J. and Rogers, C., Dual Emission Laser Induced Fluorescence for Direct Planar Scalar Behavior Measurements, Experiments in Fluids, 25 (1998), 1-15.

Hong, S. D., et al., Evaluation of a Reacting Jet Mixing by LIF Technique, Proc. 6th Asian Symposium on Visualization, (2001), 153-155.

Koochesfahani, M. M. and Dimotakis, P. E., Mixing and Chemical Reactions in a Turbulent Liquid Mixing Layer *J. Fluid*

Mech., 170 (1986), 83-112.
Nagata, K. and Komori, S., The Effects of Unstable Stratification and Mean Shear on the Chemical Reaction in Grid Turbulence, *J.* Fluid Mech., 408 (2000), 39-52.
Okamoto, K., et al., Quantitative Visualization of the Chemical Reacting Jet, Proc. 2nd Japan-Korea Symp. On Nuclear *Thermal Hydraulics and Safety,* (2000), 53-57.
Sasaki, T, Visualization Study on Chemical Reacting Flow using LIF, Master Thesis of Tokyo Univ., *JAPAN.* (2000).

Author Profile

SeongDae Hong: He received his M.S. degree in Mechanical Engineering in 2000 from Korea Maritime University. He is working in Nuclear Engineering Research Laboratory, University of Tokyo as a Ph. D candidate since 2000. His research interests are Chemically reacting jet with PIV and LIF.

Koji Okamoto: He received his MSc(Eng) in Nuclear Engineering in 1985 from University of Tokyo. He also received his Ph.D in Nuclear Engineering in 1992 from University of Tokyo. He worked in Department of Nuclear Engineering, Texas A & M University as a visiting associate professor in 1994. He works in Nuclear Engineering Research Laboratory, University of Tokyo as an associate professor since 1993. His research interests are Quantitative Visualization, PIV, Holographic PIV Flow Induced Vibration and Thermal-hydraulics in Nuclear Power Plant.

Hyun Jung Kim: He received his M.S. degree in Mechanical Engineering in 1996 from Hanyang University. He received his Ph.D. in Mechanical Engineering in 2001 from Texas A&M University. He is working in Nuclear Engineering Research Laboratory, University of Tokyo as a research associate since 2001. His research interests are micro scale heat and mass transfer and measurement with Micro PIV, LIF

Yasuhiko Sugii: He received his Ph. D degree from Osaka prefecture University in 2000. He worked in Kao corporation from 1992 to 1995, and he was a post-doctoral fellow in Nuclear Engineering Research Laboratory, University of Tokyo from 2000 to 2002. He works as a Research Associate in Nuclear Engineering Research Laboratory, University of Tokyo since 2002. His research interests are in the image measurement of flow field, bio-fluid mechanics in blood flow and micro flow dynamics in MEMS and Micro TAS.

Haruki Madarame: He received his master's degree in Mechanical Engineering in 1972 from University of Tokyo. He worked at Toshiba Research and Development Center from 1972 to 1975. He got his doctor's degree in Mechanical Engineering in 1976, and began to work in Nuclear Engineering Department, University of Tokyo as an associate professor. He has been a professor of the Nuclear Engineering Research Laboratory, the University of Tokyo since 1990. His current interests include thermal hydraulics, flow-induced oscillations, and nuclear reactor safety.